

1 **Toxicity of differently sized and coated silver nanoparticles to the bacterium**
2 ***Pseudomonas putida***

3
4 Marianne Matzke^{1*}, Kerstin Jurkschat² & Thomas Backhaus¹

5 ¹University of Gothenburg, Department of Biological and Environmental Sciences,
6 Carl Skottsbergs Gata 22 B, 40530 Göteborg/Sweden

7 ²Department of Materials, Oxford University Begbroke Science Park, Begbroke Hill,
8 Yarnton, Oxford OX5 1PF, United Kingdom

9 *Present address corresponding author: Centre for Ecology and Hydrology, Natural Environment
10 Research Council, Hails Section, Maclean Building, Benson Lane, Crowmarsh Gifford Wallingford,
11 OX10 8BB, United Kingdom, martzk@ceh.ac.uk

12
13 **Abstract**

14 Aim of this study was to describe the toxicity of a set of different commercially
15 available silver nanoparticles (AgNPs) to the gram-negative bacterium *Pseudomonas*
16 *putida* (growth inhibition assay according to ISO 10712) in order to contribute to their
17 environmental hazard assessment. Different AgNP sizes and coatings were selected in
18 order to analyze whether those characteristics are determinants of nanoparticle
19 toxicity. Silver nitrate was tested for comparison. In general *Pseudomonas putida*
20 reacted very sensitive towards the exposure to silver, with an EC₁₀ value of
21 0.058 µg/L for AgNO₃ and between 0.15 and 4.93 µg/L for the different AgNPs (EC₅₀
22 values 0.16 µg/L for AgNO₃, resp. between 0.25 and 13.5 µg/L for AgNPs). The
23 results indicate that the toxicity is driven by the Ag⁺ ions, implying that an
24 environmental hazard assessment for microorganisms based on total silver
25 concentration and the assumption that AgNPs dissolve is sufficiently protective. The
26 characterization of particle behavior as well as the total and dissolved silver content in

the medium during the exposures was not possible due to the high sensitivity of *Pseudomonas* (test concentrations were well below detection limits), indicating the need for further development in the analytical domain.

1. Introduction

Metal and metal oxide Nanoparticles (NPs) are currently the particles with the highest production volume with an estimated annual use of 320 tons nanosilver (Nowack, Krug and Height, 2011). According to the Woodrow Wilson Inventory (<http://www.nanotechproject.org>, February 2013) silver nanoparticles (AgNPs) are the dominating nanomaterial in consumer products. In order to assess whether a significant environmental exposure might result from the continuously increasing use of AgNPs several studies modeled predicted environmental silver concentrations, based on production volumes, the AgNP content in typical consumer products, clearance rates in sewage treatment plants (STPs) and average water flows. The resulting predicted environmental concentrations of AgNPs in surface waters were in the range between 0.01 and 80 ng Ag/L (Mueller and Nowak, 2008). Effluents from STPs are expected to contain higher concentrations in the range of 38-127 ng Ag/L (Gottschalk et al., 2010; Gottschalk et al., 2009). Also the steady release of silver via abrasion, wash water and sewage treatment plants bears the risk of a significant accumulation of silver in aquatic and terrestrial ecosystems (Nowak, 2010). A recent study from Mitrano and co-workers (2012) found that the effluents of a sewage treatment plant in Boulder, Colorado (USA) contained concentrations of 100 ng/L AgNPs (determined by single particle ICP-MS) in the presence of 60 ng/L dissolved silver.

51 The driving factor for using AgNPs in a broad range of health care and consumer
52 products such as bandages, surface coatings, medical equipment, food packaging,
53 functional clothes and cosmetics is their broad-spectrum antimicrobial properties
54 (D'Britto et al., 2011; Marambio-Jones and Van Hoek, 2010). However, the
55 beneficial antimicrobial effects of silver nanomaterials might become problematic
56 when silver is released into the environment as its bactericidal effects might have
57 negative consequences for ecosystem health impairing critical bacteria-driven matter
58 cycles (nutrients, degradation of organic matter). Bacteria are usually amongst the
59 most sensitive species, although - depending on the tested bacterial species, biotest
60 system or the specific particle type - toxicity values range from ng Ag/L to mg Ag/L
61 (e.g. Fabrega et al., 2011, Marambio-Jones and Van Hoek, 2010).

62 The antimicrobial activity of silver can be mainly attributed to interactions of silver
63 ions with thiol groups of cellular proteins, leading to their inactivation. Processes such
64 as cell respiration, ion transport across membranes, (Marambio-Jones and Van Hoek,
65 2010), breakdown of ATP production and the ability of the DNA to replicate (Feng et
66 al., 2000) are affected as a consequence. However, the mechanisms of toxic action for
67 AgNPs are still not very well defined (Fabrega et al., 2011). In particular it is still not
68 clear whether the effects of AgNPs are dominated by released silver ions or are
69 caused by the unique properties of the particles themselves. Literature provides
70 evidence for both particle dominated (Sheng and Yang, 2011; Morones et al., 2005)
71 as well as silver ion dominated toxicity (Navarro et al., 2008). In summary, the
72 following three mechanisms are currently suggested in the literature to be mainly
73 responsible for the antimicrobial activity of silver and AgNPs:

- 74 i) The release of silver ions from silver nanoparticles and the resulting uptake of
75 these ions into the cells, leading to similar toxicological consequences as an

exposure to silver salts, in particular the generation of reactive oxygen species (ROS). ROS are in general produced by metals in the presence of dissolved oxygen and cause DNA damage, uncontrolled oxidation of proteins, breakdown of membrane functions, and as a result damage to cellular structures such as mitochondria.

ii) Direct interactions of the AgNPs with the membrane lipids leading either to membrane damage and/or inducing the uptake of the particles into the cells, where they function as deposits for the release of silver ions. This was demonstrated especially for the effects of small AgNPs (1-10 nm) on gram-negative bacteria (e.g. *Escherichia coli*, *Vibrio cholera*, *Pseudomonas aeruginosa*, Morones et al., 2005).

iii) Interaction of AgNPs with sulfur containing membrane proteins of the membrane cells which will lead to a disruption of the membran structure.

The huge diversity of bacterial physiology and morphology is a substantial challenge for investigating the mode of action of AgNPs. Evidence from literature indicates that gram-negative bacteria are in general more sensitive to the effects of silver and AgNPs than gram-positive bacteria (Fabrega et al., 2011), which might be due to the thinner peptidoglycan layer found in the cell wall of gramnegative species

For these reasons *Pseudomonas putida*, a gram-negative, aerobic, mobile rod which is ubiquitously distributed in soils and surface waters, was selected as a test species in the present study. Aim of the study was to describe the toxicity of a set of diverse AgNPs to this organism in order to contribute to the environmental hazard assessment of AgNPs. We tested AgNPs with different sizes and coatings in order to analyze whether those characteristics are determinants of nanoparticle toxicity. Silver nitrate was tested for comparison.

We used the growth inhibition assay with *Pseudomonas putida*, which is standardized according to ISO 10712 (1995) and is commonly used for hazard assessments of other pollutants such as e.g. pharmaceuticals in the environment (Zounekova et al., 2007) or metals (Teodorovic et al., 2009). However, despite its widespread use and the general high sensitivity of bacteria to the various forms of silver, *Pseudomonas* has to our knowledge not been used previously for the hazard characterization of AgNPs.

2. Materials and Methods

All selected AgNPs are available from commercial sources, but were partly acquired through the FP7 project NanoFATE (nAg1 and nAg7) and the German R&D project UMSICHT (nAg2 and nAg3), see acknowledgements. An overview of suppliers, reported primary particle size, reported silver content and coating is given in Tab. 1.

2.1. Preparation of test dispersions

All particles were delivered in aqueous dispersions, except nAg7 (powder) and nAg3 (viscous liquid). Pre-dilutions were made in Milli-Q water, if necessary. nAg7 and nAg3 were weighed and dispersed in Milli-Q water for preparing the stock dispersion. nAg7 was prepared according to the protocol given by the suppliers, i.e. 30 seconds sonification after mixing with Milli-Q water to separate micron sized agglomerates. The nAg3 dispersion contained an unknown stabilizing agent, which was also tested purely without any nanoparticles, in order to determine its toxicity. The stabilizing agent did not cause any toxicity up to a concentration that is present in the nAg3 dispersion at 100% toxicity (data not shown).

Tab. 1: Properties of the tested AgNPs

2.4. Nanoparticle characterization

An initial range finding proved that both the silver nitrate as well as the silver nanoparticles caused strong toxic effects to *Pseudomonas putida*. It was hence neither possible to describe particle behavior nor could dissolved silver concentrations be determined during the tests, as particle numbers and silver concentrations were below the limit of detection and quantification for ICP-MS analyses and the NanoSight Nanoparticles Tracking Analysis (NTA). Hence, stock dispersions were analyzed prior to the experiments with transmission electron microscopy to ascertain information about nanoparticle quality, shape and the homogeneity of the dispersion. Diluted stock dispersions in Milli-Q water, which formed the basis for the dilution series in the actual test medium, were checked for the particle behavior and the particle concentration applying NTA.

2.4.1. Transmission Electron microscopy (TEM)

Experiments were carried out on a JEOL 2010 analytical TEM (JEOL Ltd, Japan), equipped with a LaB₆ electron gun and operated between 80 and 200kV. Samples were dispersed in water and a drop of the dispersion was deposited on a holey carbon coated copper TEM grid and dried at room temperature for several hours before examination.

2.4.2. NanoSight Nanoparticle Tracking Analysis (NTA)

Particle concentrations and size distributions of the stock dispersions were checked with NTA, using a LM10HSBF (NanoSight Ltd, Amesbury United Kingdom) equipped with a 405nm laser and an EMCCD camera.

2.2. Growth inhibition assay with *Pseudomonas putida*

Pseudomonas putida (DSM 50026) was purchased freeze dried from the German Collection of Microorganisms and Cell Cultures (DSMZ) in Braunschweig, Germany. All components for preparing the bacterial culture and test media were purchased from Sigma-Aldrich (Stockholm, Sweden). The growth inhibition assay was performed according to ISO guideline 10712 (1995). For this purpose the initial bacteria culture was transferred into 200 mL sterilized culture medium (detailed information on the medium composition is given in the supporting information, table 2) in Erlenmeyer flasks. Optical density was measured daily at 596 nm. As soon as the culture reached an optical density of 0.2, which is indicative of the late exponential growth phase, it was diluted by a factor of 1000. This daily procedure ensured continuous exponential growth. Tests were carried out in 20 mL glass scintillation vials (Wheaton, VWR 218-2245, Sweden) using test medium (details given in table 2 supporting information) with a test incubation time of 16 hours on a shaking unit with a shaking speed of 150 rpm. Both media – culture and test medium – were prepared fresh every day using sterilized Milli-Q water.

2.3. Determination of concentration-response curves

For all compounds we determined the full concentration-response curve (0-100% effect) in at least two independent experiments. Results were pooled for the final determination of the concentration response relationships. These were modeled following the strategy described in Scholze et al. (2001), and a series of 12 different models were fitted to each data set. The best-fitting model was selected on the basis of the absolute errors and from a visual inspection of the residuals.

175 Frequently the effects at high concentrations were higher than 100%, i.e. the optical
 176 density after the exposure is below the optical density at the beginning of the
 177 experiment. This indicates that the cells undergo lysis. In order to account for this, the
 178 concentration-response models $f(x)$ – which are confined to the range of 0% to 100%
 179 effect – were extended as follows:

$$180 \quad f(x)_{modified} = \theta_{min} + (\theta_{max} - \theta_{min}) \times f(conc)$$

181 Details on the finally selected models and the corresponding parameter estimates are
 182 provided in the supporting information, table 1.

183 Effect concentrations (EC_{05} , EC_{10} and EC_{50}) were derived from the corresponding
 184 inverses of these function and the 95% confidence intervals (CI) were estimated using
 185 the standard Wald-based approach of SAS (Vers. 9.2, SAS Institute, Cary, USA).

186 All concentration-response calculations were based on the TEM-determined size
 187 distribution and the NTA-determined particle numbers, assuming a spherical shape of
 188 the particles.

189

190 **3. Results**

191 We first present the results from the particle characterization, and then provide details
 192 on the toxicity of the different particles to *Pseudomonas putida*.

193

194 **3.1 Nanoparticle characterisation by Transmission Electron microscopy (TEM)**

195 The TEM micrographs of all tested particles are shown in Fig. 1.

196

197 Fig. 1: TEM micrographs of the different silver nanoparticle dispersions.

198 a) nAg1, 3-8 nm, no coating b) nAg2, 10 nm, no coating c) nAg3, 20 nm, no coating d) nAg4, 20 nm,
 199 citrate coated e) nAg5, 20 nm, tannic acid coated f) nAg6, 40 nm, citrate coated g) nAg7, 50 nm,
 200 powder, dispersed in Milli-Q water

The TEM micrographs generally revealed well defined homogenous spherical particles within the anticipated size range (Fig. 1 a-g), with the exception of the nAg7 particles (Fig 1g) which show rather heterogeneous shapes and a broad size distribution. The nAg2 dispersion (Fig. 1 b) consisted of spherical particles but with a broad size range distribution of the primary particles (10 – 50 nm). The TEM picture of the nAg5 AgNPs shows unexpectedly a dark inner core which was identified as a gold core by Energy dispersive X-ray spectroscopy.

As the effect concentrations listed in table 3 are based on total silver and the assumption that the particles consist of silver only and are spherical, the values presented for nAg5 are an underestimation. That is, the actual silver concentration in the medium resulting from the nAg5 dissolution is lower than calculated, as a consequence of the gold core. The listed effect concentrations are likely only a rough estimate for the nAg7 particles, because of their pronounced dispersion heterogeneity.

3.2. Nanoparticle Tracking Analysis (NTA)

Particle concentrations and average particle sizes of the Milli-Q stock dispersions obtained with Nanoparticle Tracking Analysis (NanoSight) are presented in Tab. 2.

The average size of the Ted Pella, Inc. (nAg4, nAg5), British Biocell International (nAg6) and nAg3 particles were in accordance with supplier provided information. nAg2 particles, however, had an actual (NTA-determined, data not shown) size of 53 nm instead of the nominal 10 nm, corresponding to the heterogeneous size distribution of 10 to 50 nm that was observed for the primary particles in the TEM (Fig. 1 b, Tab.2).

225 Also the nAg1 particles were bigger than anticipated (NTA determined 63 nm instead
226 of 3-8nm, NTA data not shown) in average, which can be attributed to loose
227 agglomerates of the 3-8mm primary particles (Fig. 1 a).

228 Tab. 2: Size and particle concentration of the diluted AgNP stock dispersions (in Milli-Q) as
229 determined from TEM and NanoSight Nanoparticle Tracking Analysis (NTA)

230

231

232 3.1. Toxicity to *Pseudomonas putida*

233

234 Tab. 3: EC₀₅, EC₁₀ and EC₅₀ values in [µg/L] total silver. Details on parameter estimates and
235 concentration-response models are given in the supporting information, Tab. 1.

236 *values in brackets denote approximate 95% confidence intervals

237

238 Exposure to AgNO₃ as well as AgNPs caused strong toxicity to *Pseudomonas*. In
239 some cases growth inhibitions higher than 100 % were observed, indicating cell lysis.
240 Reliable concentration-response relationships could be determined for all particles,
241 with EC₀₅, EC₁₀ and EC₅₀ values in the low µg/L range (table 2).

242 AgNO₃ is the most toxic agent tested (EC₁₀ = 0.058 µg/L), although the toxicity of
243 nAg3 and nAg5 reaches almost similar levels (nAg3, EC₁₀ = 0.15µg/L, and nAg5,
244 EC₁₀ = 0.34 µg/L). The other particles were less toxic, with 10 to 85 times higher
245 EC₁₀ values (table 2).

246

247 4. Discussion

248 Silver is known to be highly toxic to aquatic wildlife. In fact, the metal is second only
249 to mercury in its toxicity (Fries et al., 2010) and its toxicity has been described in a
250 broad range of studies with vertebrates and invertebrates alike. Fabrega and co-
251 workers (2011) summarized recent studies on the toxicity of silver nanoparticles in

252 aquatic ecosystems and describe a broad range of effect concentrations, ranging from
 253 several ng Ag/L (zebrafish embryos, Yeo and Yoon, 2009) to mg Ag/L (zebrafish,
 254 Griffitt et al., 2008 and 2009) for fish alone. For other aquatic organisms the span is
 255 equally wide, ranging from 0.46 mg/L for *Ceriodaphnia* (Griffitt et al., 2009) to 2.15
 256 ng/L for the diatom *Thalassiosira weissflogii* (Miao et al., 2009). Prokaryotic
 257 organisms such as *Escherichia coli*, nitrifying bacteria, *Pseudomonas fluorescence* or
 258 *Pseudomonas putida* biofilms tend to belong to the more sensitive organism groups,
 259 EC₅₀ values are typically in the µg Ag/L range (Fabrega et al., 2009, 2011).

260
 261 Especially the effects of silver to *Escherichia coli* have been studied intensively, with
 262 the bulk of the recorded EC₅₀ values falling into the range of 1 to 10 mg/L (Hwang et
 263 al., 2008, Lok et al., 2006, Morones et al., 2005), although Pal and coworkers (2007)
 264 recorded lower EC₅₀ values between 0.1-10 µg/L, and Lok et al (2006) even reported
 265 EC₅₀ values between 43 - 86 ng/L. The reasons behind this broad range of reported
 266 EC₅₀ values are currently unknown, a clear relation between acute and chronic effects
 267 on *Escherichia coli* seems to be absent.

268
 269 Toxicity to bacteria is also heavily influenced by the life style of the exposed bacteria,
 270 as demonstrated by Sheng and co-workers (2011) who comparatively analyzed the
 271 toxicity of AgNPs on bacterial biofilms and planktonic bacteria. They found only low
 272 toxicities when exposing biofilms (effects only visible at concentrations > 200 mg/L
 273 after 24 hours incubation time) but with a dramatic increase in toxicity when the
 274 bacteria were extracted from the biofilm and tested in their planktonic form. Then
 275 nearly all bacteria died already at an exposure of 1 mg/L over only one hour

incubation time. This corresponds well with the high sensitivity of a planktonic bacterium after an exposure of 16 hours, as reported in the present study.

Radniecki and co-workers (2011) found 20 nm particles to be more toxic than 80 nm particles, which was attributed to the higher release rate of Ag^+ ions from the smaller particles with a bigger surface area per mass. This hypothesis was also in concordance with studies from Pal et al., (2007) and Sadeghi et al., (2012) who both investigated the influence of different nanoparticle shapes (rods, triangles, spherical particles) on bacterial toxicity. Both conclude that certain shapes increase or decrease the toxicity of AgNPs which can be explained by an increased or decreased surface area of the particles releasing more or fewer Ag^+ ions.

The assumption that the smallest primary particles were most toxic did not hold true in the present study, as the nAg1 particles with a nominal diameter of 3-8 nm only had an intermediate toxicity (EC_{50} value = 3.4 $\mu\text{g/L}$), far lower than the 20nm particles nAg3. However the fact that the nAg1 particles were present in loosely bound agglomerates already in the stock suspension will most likely have led to a reduced Ag^+ ion release into the medium (due to the lower volume to surface ratio) and therefore to the observed apparently reduced toxicity. The same holds true for the nAg2 particles. Using the NTA data, which sized nAg1 as well as nAg2 particles in the range >50nm diameter, i.e. similar to the nAg7 particles, would result in a toxicity order of $\text{nAg3} > \text{nAg7} \sim \text{nAg1} \sim \text{nAg2}$, i.e. an increasing NTA-determined size leads to a decreasing toxicity of the uncoated particles tested.

Tannic acid and citrate are both relatively loosely attached coatings and can probably be easily removed or exchanged with proteins and other compounds present in the growth medium. Nevertheless the coating seems to stabilize the particles to a certain point preventing them from agglomeration and therefore increasing their dissolution rate. Results from Ahmed et al. (2010) investigated the influence of the coating on the AgNP toxicity and found that coated AgNPs caused more severe DNA damage than uncoated particles, probably caused by the lower surface area of the uncoated particles as a result of their agglomeration. A similar result was also found by Aranout and co-workers (2012) who investigated the effects of three different coatings (citric acid, gum arabicum (GA) and polyvinylpyrrolidone (PVP)) coated AgNPs and found that the citrate and the GA clearly increased the toxicity towards *Nitrosomonas europaea* probably due to a higher Ag^+ ion release rate. Our findings also point to a complex interaction between coating and toxicity: while the most toxic particles (nAg3) were uncoated, citrate coated particles of the same diameter (nAg4) were less toxic but tannic acid coated particles (nAg5) were, again, more toxic, despite the fact that those particles contain a gold-core and hence the total silver based effect concentrations in table 3 are an underestimation for nAg5. So far it is unclear whether the observed high toxicity of the nAg5 particles is, at least partly, caused by particle-specific effects of the insoluble gold core.

There seems to be a general agreement in the literature that the resulting concentration of silver ions is the most important determinant for the toxicity of silver particles. However, there is an ongoing discussion in the literature on whether and to what extent particle specific effects contribute to the overall toxicity. Morones and co-workers (2005), for example, demonstrated that selected gram-negative bacteria (e.g.

Escherichia coli, *Vibrio cholera*, *Pseudomonas aeruginosa*) react with the formation of so-called low molecular weight regions (a defense mechanism of to protect the DNA) to an exposure to silver nitrate, but not to AgNPs. Also Ortega-Calvo and co-workers (2011) found particle related effects on the tactic motility of *Pseudomonas putida*: the bacteria were repelled by AgNPs but not by AgNO₃, suggesting a particle specific effect. On the other hand, Xiu and coworkers recorded the toxicity of AgNPs to *Escherichia coli* under strictly anaerobic conditions in order to avoid Ag oxidation and inferred that “Ag⁺ is the definitive molecular toxicant”, in particular because the toxicity of various differently sized, shaped and coated particles strictly followed the concentration-response pattern observed for AgNO₃ (Xiu et al, 2012). Similar conclusions were drawn by Radniecki and coworkers (2011).

The results presented in this study (table 3, figure 2) clearly show that ionic silver is the most toxic form of silver, i.e. that silver ions dominate the overall toxicity. However, the toxicity of the different particles is clearly different. Whether this is caused by different dissolution kinetics, aggregation, uptake or even particle-specific effects is a subject for further studies, as soon as sufficiently sensitive analytical techniques are available.

Fig. 2: Graphical overview of the recorded EC₀₅ values for AgNO₃ and the seven tested AgNPs in this study in relation to the silver concentrations found in surface waters of various geographical regions (numerical data and references for the surface water concentrations of the silver are given in the supporting information)

Figure 2 also provides an overview of silver concentrations found in surface waters of various regions (all numerical data and references are provided in the supporting information). The highest silver concentrations of more than 100 µg/L total silver

were detected in Ghanaian estuaries near silver mining areas (Essumang & Nortsu, 2008), closely followed (surprisingly) by silver monitoring data from German rivers, compiled by Hund-Rinke et al (2008). Here, concentrations of up to 65 $\mu\text{g/L}$ silver were detected in Bavaria in 2006 (mean=1.17 $\mu\text{g/L}$, the average concentrations in various German counties in 2000-2007 fall between 0.05 – 1.17 $\mu\text{g/L}$). Ahmed and coworkers also determined silver concentrations in the $\mu\text{g/L}$ range in a heavily industrialized area in Bangladesh (max=14.9 $\mu\text{g/L}$, mean=5.23 $\mu\text{g/L}$) (Ahmed et al., 2012). However, most other analytical surveys reported concentrations in surface water in the ng/L range (see Fig 2). Roditi et al. even determined dissolved silver concentrations below 0.1 ng/L for lake Erie, Ontario and the Niagara and Hudson rivers, corresponding to total (unfiltered) concentrations between 1.3 and 8.3 ng/L (Roditi et al, 2000). However, it should be pointed out that the analytical survey was conducted already in 1997 and it is not known whether the continuously increasing use of silver and silver nanoparticle containing products has led to increased silver concentrations in those river systems since then.

This extremely broad range of environmental silver concentrations, which span six orders of magnitude, indicates that a general conclusion on whether the current use of silver and silver nanoparticles constitutes an environmental risk cannot be drawn. A case-by-case evaluation is needed instead. The toxicity data that were recorded in the present study only differ by a factor of less than 100, small in comparison to the dynamics in environmental concentrations. However, a good proportion of analytical determined silver concentrations are in a range that directly affects the growth pattern of *Pseudomonas* (Figure 2), a common environmental bacterium.

5. Conclusions

The objective of this study was to contrast the effects of different silver nanoparticle sizes (3-8 nm, 10 nm, 20 nm, 40 nm and 50 nm) as well as different coatings (uncoated, citrate coating and tannic acid coating) with the toxicity of ionic silver (silver nitrate) to the gram-negative bacterium *Pseudomonas putida*.

Our results show no simple clear-cut relation between the toxicity of the different particles and their shapes and coatings. They, however, strongly indicate that the overall toxicity is driven by Ag^+ ions. The final toxic effect of a given AgNP can hence be assumed to be linked to the actual Ag^+ ion release rate from the particles during the test, which in turn is dependent on the coating (preventing agglomeration), the primary particle size (higher release rate from smaller particles), the agglomeration status, the medium components and the exposure conditions (e.g. light, oxygen concentrations) (Fabrega et al., 2011; Marambio-Jones and von Hoek, 2010). However the determination of the overall agglomeration behavior and ion release kinetics remains highly challenging for test organisms as sensitive as *Pseudomonas putida*. Detection limits of the available characterization equipment, in particular in complex growth media, prevent a real time analysis of the exposure situation and definite conclusions on the particle behavior.

As the free ions generally represent the most toxic silver form, an environmental hazard assessment for aquatic microorganisms that is based on the total silver content should be sufficiently protective. However, the hazard profiles of free silver and silver nanoparticles might differ substantially for higher organisms which might take up particles directly e.g. via gills, which would then deliver silver ions directly to certain tissues. Available data seem to indicate that microorganisms are generally the most

402 sensitive organismic group, i.e. they would be driving the hazard assessment. In this
403 context more data on the toxicity of silver and silver nanoparticles to algae, one of the
404 cornerstones of the standard “base set” of ecotoxicological data, used e.g. within
405 REACH or the Biocide Regulation (EU) 528/2012, would improve our current
406 understanding of the environmental risks of silver and silver nanoparticles.

407

408

409 **Acknowledgements**

410 The authors gratefully thank the following projects for financial support:

411 The strong research environment Nanosphere (Center for Interaction and Risk studies
412 in Nano-Bio-Geo-Socio-Techno-sphere interfaces) funded by FORMAS, Sweden

413 The EU-project NanoFate (Nanoparticle Fate Assessment and Toxicity in the
414 Environment, NMP4-SL-2010-24773

415 And the following people for their support and helpful discussions:

416 Åsa Arrhenius (Department of Biological and Environmental Sciences, Gothenburg
417 University) for her support with the growth inhibition assay with *Pseudomonas*
418 *putida*.

419 Mark Ware from NanoSight for recording the NTA videos for the determination of
420 the particle concentrations and particle sizes.

421 Jurgen Arning und Juliane Filser from the Center of Environmental Research and
422 sustainable Technologies for supplying the NM-300K and PL-Ag-S10 silver
423 nanoparticles in the context of the following project: Hazard assessment for silver
424 nanomaterials in the environment (UMSICHT), funded by the Bundesministerium für
425 Bildung und Forschung (BMBF), Germany, 03X0091

426

427 Supplementary data associated with this article can be found in the online version of
428 this article in the supporting information.

429

430 **References**

431 Ahamed, M., Posgai, R., Gorey, T.J., Nielsen, M., Hussain, S.M., Rowe, J.J., 2010.
432 Silver nanoparticles induced heat shock protein 70, oxidative stress and apoptosis in
433 *Drosophila melanogaster*. Toxicol. Appl. Pharmacol. 242, 264–269.

434

435 Ahmed, G., Miah, M.A., Anawar, H.M., Chowdhury, D.A., Ahmad, J.U., 2012.
436 Influence of multi-industrial activities on trace metal contamination: An approach
437 towards surface water body in the vicinity of Dhaka Export Processing Zone (DEPZ).
438 Environ. Monit. Assess. 184 (7), 4181-4190.

439

440 Aranout, C.L., Gunsch, C.K., 2012. Impacts of Silver Nanoparticle Coating on the
441 Nitrification Potential of *Nitrosomonas europaea*. Environ. Sci. Technol. 46 (10),
442 5387-5395.

443

444 D’Britto, V., Kapse, H., Babrekar, H., Pabhune, A.A., Bhoraskar, S.V., Premnath, V.,
445 Prasad, B.L.V., 2011. Silver nanoparticle studded porous polyethylene scaffolds:
446 bacteria struggle to grow on them while mammalian cells thrive. Nanoscale. 3 (7),
447 2957-2963.

448

449 Essumang, D.K. and Nortsu, B.K., 2008. Analysis of silver in the water column of the
450 Pra and the Eture estuaries in Ghana. Chem. Ecol. 24 (4), 297-303.

451

452 Fabrega, J., Renshaw, J.C., Ead, J.R., 2009. Interactions of Silver Nanoparticles with
453 *Pseudomonas putida* Biofilms. Environ. Sci. Technol. 43, 9004–9009.

454

455 Fabrega, J., Luoma, S.N., Tyler, C.R., Galloway, T.S., Lead, J.R., 2011. Silver
456 nanoparticles: Behaviour and effects in the aquatic environment. Environ. Internat.

457 37, 517-531.

458

459 Feng, Q., Wu, J., Chen, G., Cui, F., Kim, T., Kim, J., 2000. A mechanistic study of
460 the antibacterial effect of silver ions on *Escherichia coli* and *Staphylococcus aureus*. J.
461 Biomed. Mater. Res. 52, 662-668.

462

463 Fries, R., Gressler, S., Simko, M., Gazso, A., Fiedeler, U., Nentwich, M., 2010.
464 Nanosilver. Nanotrust. Dossiers. No. 10.

465

466 Gottschalk, F., Sonderer, T., Scholz, R.W., Nowack, B., 2010. Possibilities and
467 limitations of modelling environmental exposure to engineered nanomaterials by
468 probabilistic material flow analysis. Environ. Toxicol. Chem. 29 (5), 1036-1048.

469

470 Gottschalk, F., Sonderer, T., Scholz, R.W., Nowack, B., 2009. Modelled
471 Environmental Concentrations of Engineered Nanomaterials (TiO₂, ZnO, Ag,
472 CNT, Fullerenes) for Different Regions. Environ. Sci. Technol. 43 (24), 9216-9222.

473

474 Griffitt, R.J., Luo, J., Gao, J., Bonzongo, J.C., Barber, D.S., 2008. Effects of particle
475 composition and species on toxicity of metallic nanomaterials in aquatic organisms.
476 Environ. Toxicol. Chem. 27, 1972–1978.

477

478 Griffitt, R.J., Hyndman, K., Denslow, N.D., Barber, D.S., 2009. Comparison of
479 molecular and histological changes in zebrafish gills exposed to metallic
480 nanoparticles. Toxicol.Sci. 107 (2), 404-415.

481

482 <http://www.nanotechproject.org>, June 2012

483

484 Hund-Rinke, K.C., Schlich, A., Wenzel, A., 2011. TiO₂ nanoparticles - relationship
 485 between dispersion preparation method and ecotoxicity in the algal growth test.
 486 Umweltwiss. Schadst. Forsch, 22, 517-528.

487

488 Hwang, E.T., Lee, J.H., Chae, Y.J., Kim, Y.S., Kim, B.C., Sang, B.I., 2008. Analysis
 489 of the toxic mode of action of silver nanoparticles using stress-specific
 490 bioluminescent bacteria. Small. 4, 746-750.

491

492 ISO Guideline 10712. 1995. Water quality – *Pseudomonas putida* growth inhibition
 493 test.

494

495 Lok, C., Ho, C., Chen, R., He, Q., Yu, W., Sun, H., 2006. Proteomic analysis of the
 496 mode of antibacterial action of silver nanoparticles. J. Proteome. Res. 5, 916-924.

497

498 Marambio-Jones, C., Van Hoek, E.M.V., 2010. A review of the antibacterial effects
 499 of silver nanomaterials and potential implications for human health and the
 500 environment. J. Nanopart. Res. 12, 1531–1551.

501

502 Miao, A.J., Schwehr, K.A., Xu, C., Zhang, S.J., Luo, Z., Quigg, A., 2009. The algal
 503 toxicity of silver engineered nanoparticles and detoxification by exopolymeric
 504 substances. Environ. Pollut. 157, 3034-3041.

505

506 Mitrano, D.M., Leshner, E.K., Bednar, A., Monserud, J., Higgins, C.P., Ranville, J.F.,
 507 2012. Detecting nanoparticulate silver using single-particle inductively coupled
 508 plasma-mass spectrometry. Environ. Toxicol. Chem. 31(1),115-121.

509

510 Morones, J.R., Elechiguerra, J.L., Camacho, A., Holt, K., Kouri, J.B., Ramirez, J.T.,
 511 Yacaman, M.J., 2005. The bactericidal effect of silver nanoparticles. Nanotechnology.
 512 16 (10), 2346–2353.

513

514 Mueller, N.C., Nowack, B., 2008. Environmental Impacts of Nanosilver. Environ.
515 Sci. Tech. 42, 4447-4453.

516

517 Navarro, E., Piccapietra, F., Wagner, B., Marconi, F., Kaegi, R., Odzak, N., Sigg, L.,
518 Behra, R., 2008. Toxicity of Silver Nanoparticles to *Chlamydomonas reinhardtii*. E
519 Environ. Sci. Technol., 42, 8959–8964.

520

521 Nowack, B., 2010. Nanosilver Revisited Downstream. Science. 330, 1054-1055.

522

523 Nowack, B., Krug, H. and Height, M., 2011. 120 years of Nanosilver history:
524 Implications for policy makers. Environ. Sci. Technol. 45 (4), 1177 – 1183.

525

526 Ortega-Calvo, J. J., Molina, R., Jimenez-Sanchez, C., Dobson, P.J., Thompson, I.P.,
527 2011. Bacterial tactic responses to silver nanoparticles. Environ. Microb. Reports. 3
528 (5), 526-534.

529

530 Pal, S., Tak, K.Y. and Song, J.M., 2007. Does the Antibacterial Activity of Silver
531 Nanoparticles Depend on the Shape of the Nanoparticle? A Study of the Gram-
532 Negative Bacterium *Escherichia coli*. Appl. Environ. Microb., 1712-1720.

533

534 Radniecki, T.S., Stankus, D.P., Neigh, A., Nason, J.A., Semprini, L., 2011. Influence
535 of liberated silver from silver nanoparticles on nitrification inhibition of
536 *Nitrosomonas europaea*. Chemosphere. 85 (1), 43-49.

537

538 Roditi, H.A., Fisher, N.S., Sañudo-Wilhelmy, S.A., 2000. Field testing a metal
539 bioaccumulation model for zebra mussels. Environ. Sci. Technol. 34 (13), 2817-2825.

540

541 Sadeghi, B., Garmaroudi, F.S., Hashemi, M., Nezhad, H.R., Nasrollahi, A., Ardalan,
542 S., Ardalan, S., 2012. Comparison of the anti-bacterial activity on the nanosilver

543 shapes: Nanoparticles, nanorods and nanoplates. Adv. Powder. Technol., 23 (1), 22-
 544 29.
 545
 546 Scholze, M., Boedeker, W., Faust, M., Backhaus, T., Altenburger, R., Grimme, L.H.,
 547 2001. A general best fit method for concentration-response curves and the estimation
 548 of low-effect concentrations. Environ. Toxicol. Chem. 20, 448-457.
 549
 550
 551 Sheng, Z., Yang, L., 2011. Effects of silver nanoparticles on waste water biofilms.
 552 Water Research. 45, 6039-6050.
 553
 554 Teodorovic, I., Planojevic, I., Knezevic, P., Radak, S., Nemet, I., 2009. Sensitivity
 555 of bacterial vs. acute *Daphnia magna* toxicity tests to metals. Centr. Eur. J. Biol. 4,
 556 (4) 482-492.
 557
 558 Xiu, Z.M., Zhang, Q.B., Puppala, H.L., Colvin, V.L., Alvarez, P.J., 2012. Negligible
 559 particle-specific antibacterial activity of silver nanoparticles. Nano Lett., 12 (8), 4271-
 560 4275.
 561
 562 Yeo, M.K., Yoon, J.W., 2009. Comparison of the effects of nano-silver antibacterial
 563 coatings and silver ions on zebrafish embryogenesis. Mol. Cell. Toxicol. 5, 23-31.
 564
 565 Zounková, R., Odráska, P., Dolezalová, L., Hilscherová, K., Marsálek, B., Zounkov,
 566 B., 2007. Ecotoxicity and genotoxicity assessment of cytostatic pharmaceuticals.
 567 Environ. Toxicol. Chem. 26 (10), 2208-2214.
 568
 569
 570
 571
 572
 573

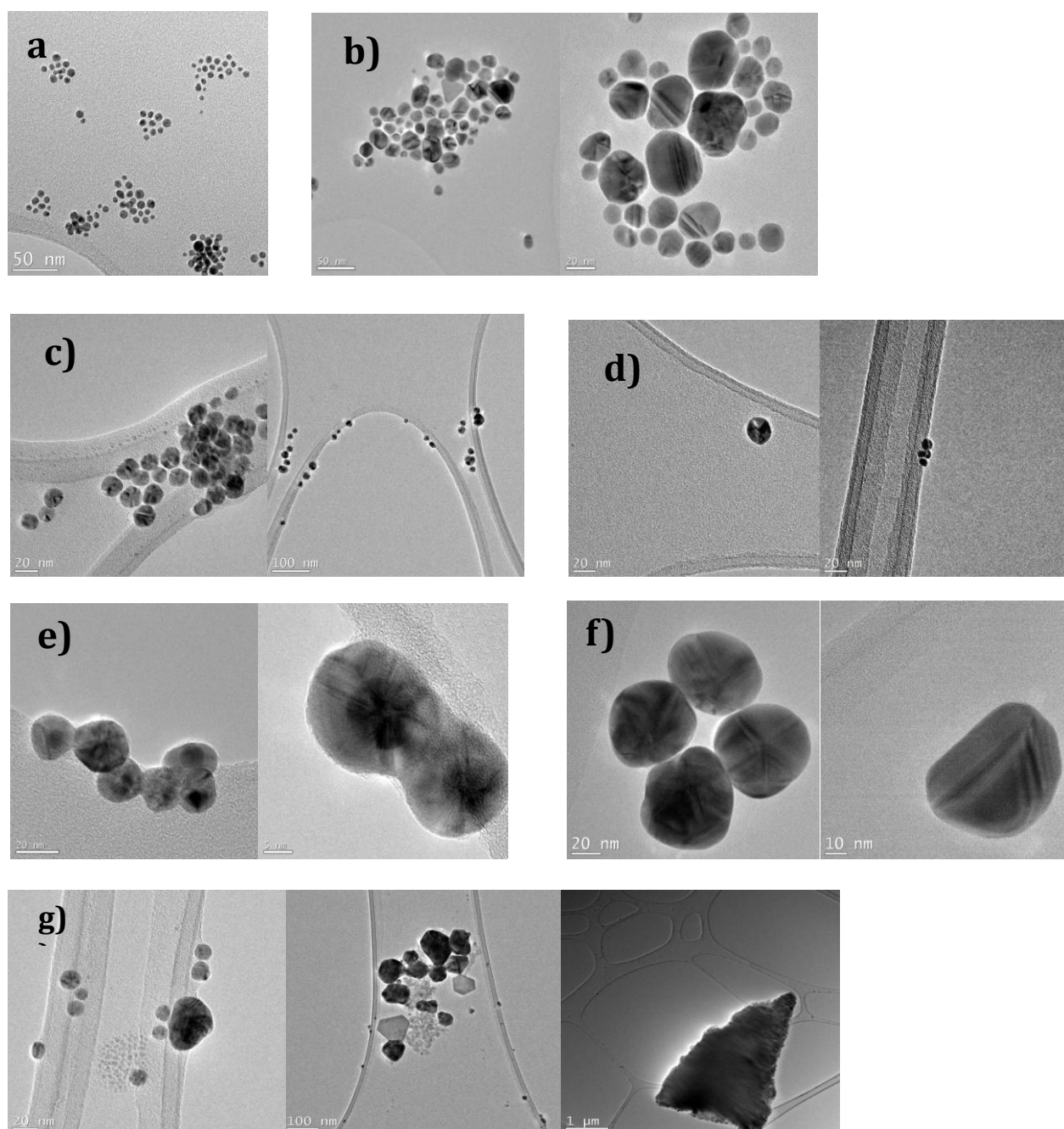


Fig. 1: TEM micrographs of the different silver nanoparticle dispersions.

a) nAg1, 3-8 nm, no coating b) nAg2, 10 nm, no coating c) nAg3, 20 nm, no coating d) nAg4, 20 nm, citrate coated e) nAg5, 20 nm, tannic acid coated f) nAg6, 40 nm, citrate coated g) nAg7, 50 nm, powder, dispersed in Milli-Q water

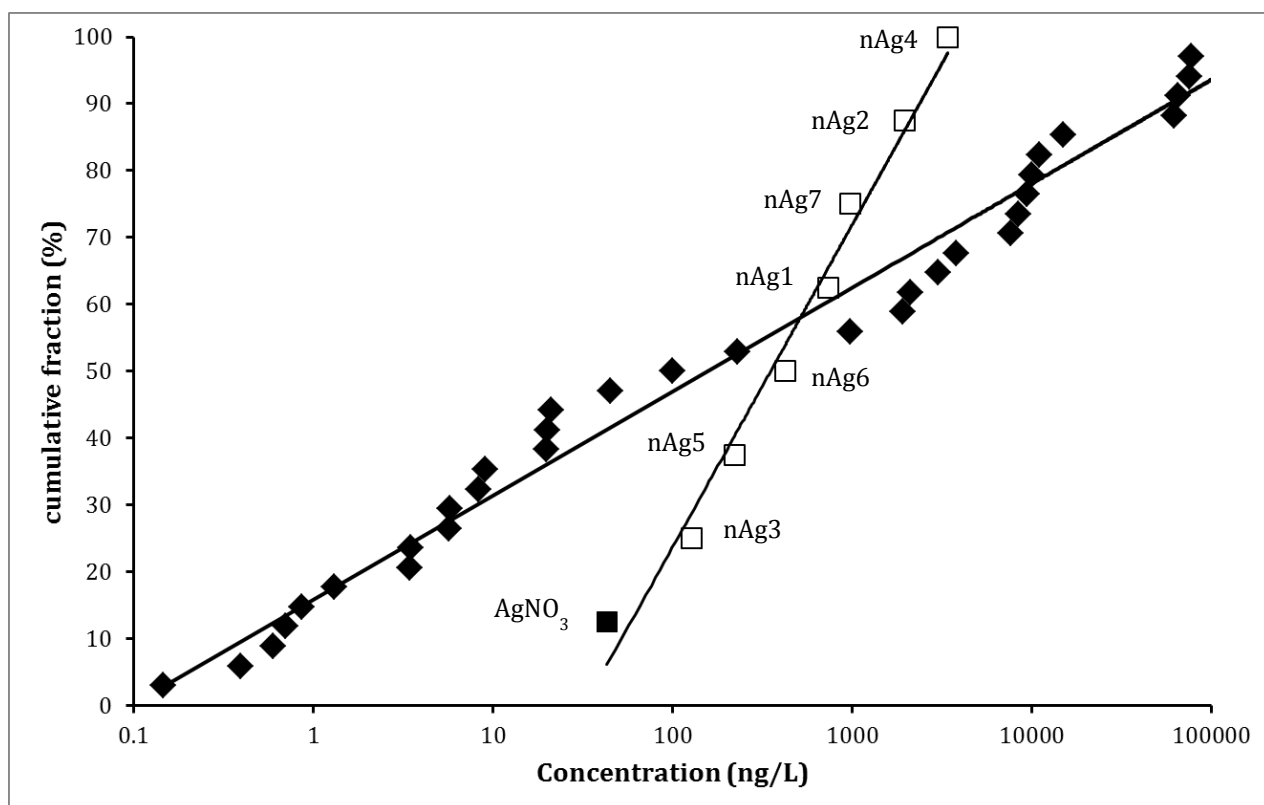


Fig. 2: Graphical overview of the recorded EC_{05} values for $AgNO_3$ and the seven tested AgNPs in this study in relation to the silver concentrations found in surface waters of various geographical regions (numerical data and references for the surface water concentrations of the silver are given in the supporting information).

608
609

Tab. 1: Properties of the tested NPs according to the suppliers information.

Acronym	Name	Supplier	Primary particle size (nm)	Coating	Particle concentration [particles/mL]	Silver concentration [ppm]	Medium
AgNO3	AgNO ₃	Sigma Aldrich, Germany	-	-	-	-	Powder
nAg1	AG7	Amepox, Poland	3-8	not specified	not specified	1000	Aqueous dispersion
nAg2	PL-Ag-S10	Plasmachem AG, Germany	10	not specified	not specified	100	Aqueous dispersion
nAg3	NM-300K	OECD WPMN program, JRC, Ispra, Italy	20	none	not specified	1000000	Aqueous dispersion stabilised with 4% Polyoxyethylene Glycerol Trioleate and Polyoxyethylene (20) Sorbitan mono-Laurat (Tween 20)
nAg4	PELCO [®] NanoXact™ (84060-20)	Ted Pella, Inc., USA	20	citrate	4.5*10 ¹¹	20	2 mM citrate buffered dispersion, pH 7.4
nAg5	PELCO [®] NanoXact™ (84160-20)	Ted Pella, Inc., USA	20	tannic acid	4.5*10 ¹¹	20	2 mM citrate buffered dispersion, pH 7.4
nAg6	Silver colloid	British Biocell International, UK	40	citrate	9*10 ⁹	n.d.	dispersed in water, no preservatives, residual chemical left from manufacture (not specified)
nAg7	AG6	NanoTrade, Czech Republic	50	none	not specified	not specified	powder

610

611

612

613

614

615

616

617

618

619

620

621

622

623 Tab. 2: Size and particle concentration of the diluted AgNP stock dispersions (in Milli-Q) as
 624 determined from TEM and NanoSight Nanoparticle Tracking Analysis (NTA)

Particle type	Average size, nm (TEM)	Particle conc. [particles/mL] (NTA)	silver conc. [ppm] based on NTA particle conc. and TEM size	nominal silver conc.[ppm]
nAg1	8	2.1×10^{14}	590	1000
nAg2	14, but between 10 – 50 nm, mostly bound in loose aggregates	9.3×10^{12}	140	100
nAg3	20	2.8×10^{15}	122505	100000
nAg4	20	1.27×10^{12}	55	20
nAg5	20	7.6×10^{11}	33	20
nAg6	40	9×10^9	2.6	3.16*
nAg7	60: primary particles between 30 – 60 nm, bound in micron-sized agglomerates, possible to resuspend with sonification	3.9×10^8	0.46	0.1

625
 626 *calculated based on the primary particle size and the particle number, no information about the silver
 627 content was given by the supplier

628 Tab. 3: Overview of EC₀₅, EC₁₀ and EC₅₀ values in [µg/L] total silver. Details on parameter estimates
 629 and concentration-response models are given in the supporting information, table 1.
 630

Particle Type	Particle size (TEM based)	Particle coating	EC ₀₅ [µg/L]	EC ₁₀ [µg/L]	EC ₅₀ [µg/L]
AgNO ₃	none	none	0.043 [0.053-0.036]	0.058 [0.071-0.05]	0.16 [0.18-1.69]
nAg1	8 nm	none	0.73 [0.94-0.59]	1.11 [1.36-0.92]	3.46 [3.84-3.10]
nAg2	14 nm	none	1.96 [-]	3.24 [3.75-2.77]	11.6 [12.5-11]
nAg3	20 nm	none	0.13 [0.15-0.11]	0.15 [0.17-0.13]	0.25 [0.28-0.26]
nAg4	20 nm	citrate	3.41 [4.82-2.59]	4.93 [6.52-3.88]	13.4 [15.3-11.6]
nAg5	20 nm	tannic acid	0.22 [0.29-0.18]	0.34 [0.41-0.28]	1.03 [1.16-0.93]
nAg6	40 nm	citrate	0.42 [0.57-0.33]	0.69 [0.86-0.55]	2.40 [2.68-2.13]
nAg7	60 nm	none	0.98 [1.43-0.71]	1.66 [2.22-1.25]	6.9 [7.95-5.90]

631